DOI: 10.1002/cphc.200((will be filled in by the editorial staff))

Electron Transfer between Hydrogen-Bonded Pyridylphenols and a Photoexcited Rhenium(I) Complex

William Herzog,[b] Catherine Bronner,[a] Susanne Löffler,[c] Bice He,[c] Daniel Kratzert,[c] Dietmar Stalke,[c] Andreas Hauser,[b] and Oliver S. Wenger*[a]

Two pyridylphenols with intramolecular hydrogen bonds between the phenol and pyridine units were synthesized, characterized crystallographically, and investigated by cyclic voltammetry and UV-vis spectroscopy. Reductive quenching of the ^{3}MLCT excited state of the [Re(phen)(CO)$_3$(py)]$^+$ complex (phen = 1,10-phenanthroline, py = pyridine) by the two pyridylphenols and two reference phenol molecules was investigated by steady-state and time-resolved luminescence spectroscopy, as well as by transient absorption spectroscopy. Stern-Volmer analysis of the luminescence quenching data provides rate constants for the bimolecular excited-state quenching reactions. H/D kinetic isotope effects (KIEs) for the pyridylphenols are on the order of 2.0, and the bimolecular quenching reactions are up to 100 times faster with the pyridylphenols than with the reference phenols. This observation is attributed to the markedly less positive oxidation potentials of the pyridylphenols with respect to the reference phenols (ca. 0.5 V), which in turn is caused by proton-coupling of the phenol oxidation process. Transient absorption spectroscopy provides unambiguous evidence for the photogeneration of phenoxyl radicals, i. e., the overall photoreaction is clearly a PCET process

Introduction

The tyrosine Z (Tyr$_Z$) / histidine 190 (His190) pair of photosystem II is one of the best-known hydrogen-bonded phenol systems in chemistry.[1] Numerous experimental and theoretical investigations have been geared at understanding the proton-coupled electron transfer (PCET) chemistry of the Tyr$_Z$ / His190 reaction couple, many of them focusing on simple artificial model compounds in which a phenol unit can form intramolecular hydrogen bonds to a nitrogen base.[2] A wide range of experimental methods has been applied, including EPR,[3] electrochemical,[4] and optical spectroscopic studies.[5] However, in most cases the phenol oxidation process involves oxidants which are in their electronic ground states, and there are comparatively few studies in which the oxidant is an electronically excited molecule.[5b, 6]

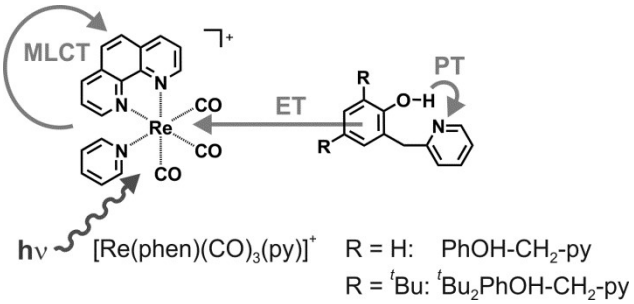

Scheme 1. Molecular structures of the photosensitizer/quencher pairs with the two hydrogen-bonded phenol molecules of central interest to this study; hν = light excitation; MLCT = metal-to-ligand charge transfer excitation; ET = electron transfer; PT = proton transfer.

Against this background we deemed it interesting to explore the photoredox chemistry between hydrogen-bonded phenol molecules and a photoexcited rhenium(I) tricarbonyl diimine complex which is known to be a potent excited-state oxidant.[6e, 7] The molecular structures of our model systems are shown in Scheme 1. The rhenium(I) complex has a 1,10-phenanthroline (phen) and a pyridine (py) ligand in addition to the three carbonyls, the phenol reaction partners have pendant pyridine units that are connected via a –CH$_2$– group in order to disrupt π-conjugation between the two aromatic subunits. One of the phenols contains no further substituents (PhOH-CH$_2$-py) while the other has *tert.*-butyl groups at the 4- and 6-positions (^{t}Bu$_2$PhOH-CH$_2$-py). We anticipated that when excited to its long-lived ^{3}MLCT state the rhenium(I) complex would be capable of inducing *inter*molecular electron transfer (ET) with the phenol, and this process should be accompanied by *intra*molecular proton transfer (PT) between the phenol and the pyridine.

The PCET chemistry of ^{t}Bu$_2$PhOH-CH$_2$-py with various

[a] *Dr. C. Bronner, Prof. O. S. Wenger*
Departement für Chemie
Universität Basel
Spitalstrasse 51, CH-4056 Basel, Switzerland
Fax: +41 (0)61 267 09 76
E-mail: oliver.wenger@unibas.ch
[b] *Dr. W. Herzog, Prof. A. Hauser*
Département de Chimie Physique
Université de Genève
30 quai Ernest-Ansermet, CH-1211 Genève 4, Switzerland
[c] *S. Löffler, Dr. B. He, D. Kratzert, Prof. D. Stalke*
Institut für Anorganische Chemie
Georg-August Universität
Tammannstrasse 4, D-37077 Göttingen, Germany

Supporting information for this article is available on the WWW under http://www.chemphyschem.org or from the author.

oxidants in their electronic ground states has been found previously to occur via a concerted proton-electron transfer (CPET) mechanism.[2e, 5c-f] Here we focus specifically on the *excited-state* PCET chemistry between $[Re(phen)(CO)_3(py)]^+$ and PhOH-CH_2-py or ^{t}Bu$_2$PhOH-CH_2-py. As reference phenols without the possibility of forming intramolecular hydrogen bonds we used ordinary phenol (PhOH) and 2,4-di-*tert.*-butylphenol (^{t}Bu$_2$PhOH).

Results and Discussion

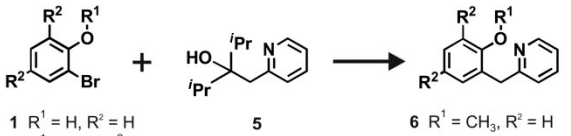

1 R^1 = H, R^2 = H
2 R^1 = CH_3, R^2 = H
3 R^1 = H, R^2 = ^{t}Bu
4 R^1 = CH_3, R^2 = ^{t}Bu

5

6 R^1 = CH_3, R^2 = H
7 R^1 = H, R^2 = H
8 R^1 = CH_3, R^2 = ^{t}Bu
9 R^1 = H, R^2 = ^{t}Bu

Scheme 2. Synthesis of the two pyridylphenols from Scheme 1.

Synthesis

The synthesis of ^{t}Bu$_2$PhOH-CH_2-py had been previously described,[5c, 5d, 5f] but in our hands a different procedure turned out to be more convenient for obtaining the two pyridylphenols from Scheme 1.[8] Our synthetic strategy is illustrated by Scheme 2 and begins with commercially available 2-bromophenols (**1** and **3**), which are methylated in order to protect the phenolic function for the subsequent reaction step. The protected phenols (**2** and **4**) are reacted with pyridine molecule **5** (which is accessible in one step from 2-picoline and diisopropyl ketone) using a palladium catalyst.[8] The coupling products (**6** and **8**) are deprotected using aqueous HBr (in the case of **6**)[9] or ethanethiol (in the case of **8**)[10] in order to obtain the final pyridylphenols (**7**, PhOH-CH_2-py and **9**, ^{t}Bu$_2$PhOH-CH_2-py).

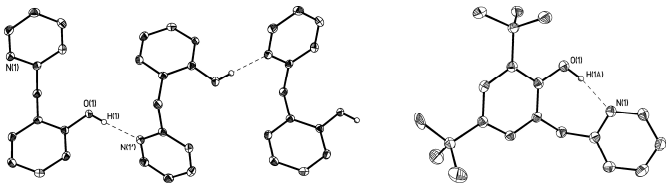

Figure 1. Crystal structures of PhOH-CH_2-py (left) and ^{t}Bu$_2$PhOH-CH_2-py (right). Anisotropic displacement parameters are depicted at the 50 % probability level. Selected bond distances and angles can be found in the supporting information.

Crystal structures

Figure 1 (left) shows the crystal structure of PhOH-CH_2-py which crystallizes in the monoclinic space group *C*2/*c* with one molecule in the asymmetric unit. The molecules in the crystal lattice of PhOH-CH_2-py are connected through intermolecular hydrogen bonds between the phenolic OH group and the nitrogen of the pyridyl ring. These bonds generate a zigzag like chain along the b axis of the crystal lattice. The position of the hydrogen atom was modeled as a riding atom with a fixed distance of 0.84 Å and a freely refined torsion angle. The resulting hydrogen bond is slightly bent with 175° for the O-H-N angle and has a H-N distance of 1.90 Å, resulting in a total O-H-N distance of 2.740(2) Å. Figure 1 (right) shows the crystal structure of ^{t}Bu$_2$PhOH-CH_2-py which crystallizes in the monoclinic space group $P2_1/n$ with one molecule in the asymmetric unit. One of the ^{t}Bu groups happens to be disordered by 5%. This molecule only forms an intramolecular hydrogen bond between H1 and N1. The hydrogen H1 was found in the difference Fourier density. Position and the isotropic vibration were refined freely with a distance restraint of 0.84(2) Å to O1. The O-H distance refined to 0.88(2) Å with a N-H distance of 1.827(16) Å and a total O-N distance of 2.6956(16) Å with an O-H-N angle of 169(2)°. Thus, there is clear evidence for hydrogen-bonding interactions in the crystal structures of PhOH-CH_2-py and ^{t}Bu$_2$PhOH-CH_2-py.[11] A structure of ^{t}Bu$_2$PhOH-CH_2-py had been previously published.[25]

Intramolecular hydrogen-bonding in solution

^{1}H NMR spectra of the two pyridylphenols in $CDCl_3$ exhibit sharp downfield resonances for the phenolic protons, specifically at 11.67 ppm for PhOH-CH_2-py and at 11.40 ppm for ^{t}Bu$_2$PhOH-CH_2-py, which is typical for intramolecularly hydrogen-bonded phenols.[12] We conclude that intramolecular hydrogen-bonds are not only present in one of our solid state structures but also in aprotic solution

Cyclic voltammetry

Figure 2 shows cyclic voltammograms of (a) ^{t}Bu$_2$PhOH, (b) ^{t}Bu$_2$PhOH-CH_2-py, and (c) PhOH-CH_2-py in dry CH_2Cl_2 in presence of 0.1 M $TBAPF_6$ electrolyte. The reversible waves at 0.0 V vs. Fc^+/Fc (dashed vertical line) are due to ferrocene, which was added in small quantities for internal voltage calibration. The voltammogram of the reference phenol (a) exhibits an irreversible oxidation wave peaking at 1.05 V vs. Fc^+/Fc which is typical for ordinary phenols because the O-H proton is lost to the bulk solution in the course of oxidation.[13]

The ^{t}Bu$_2$PhOH-CH_2-py molecule, by contrast, exhibits a voltammogram in which the oxidative peak current near 0.5 V vs. Fc^+/Fc is roughly 6 times larger than the corresponding reductive peak current. Their voltage separation is 170 mV but depends on voltage sweep rate. The voltammogram in Figure 2b is qualitatively similar to that previously reported for the same compound in CH_3CN solution.[5c] The shape of this voltammogram can be explained by the possibility of transferring the phenolic proton to the pendant pyridine base in the course of oxidation and back-transfer to the phenol unit during the subsequent reductive potential sweep. The middle between the oxidative and reductive peak currents in Figure 2b is taken as the oxidation potential of ^{t}Bu$_2$PhOH-CH_2-py (Table 1). Importantly, the oxidation potential of ^{t}Bu$_2$PhOH-CH_2-py in CH_2Cl_2 is about 0.5 V less positive than the oxidation potential of ^{t}Bu$_2$PhOH, a fact that has been previously noted for CH_3CN solution.[5c, 5d] It has been demonstrated that the unusually low oxidation potential of ^{t}Bu$_2$PhOH-CH_2-py and related hydrogen-bonded phenols is a direct manifestation of intramolecular proton transfer accompanying electrochemical phenol oxidation; hydrogen-bonding alone cannot account for the large magnitude of the oxidation potential shift.[5c, 14]

The cyclic voltammogram of PhOH-CH_2-py in Figure 2c exhibits an irreversible oxidation wave peaking at 0.66 V vs. Fc^+/Fc (Table 1). Despite the presence of an intramolecular hydrogen bond phenol oxidation is clearly irreversible in this case, possibly because of the absence of substituents at the 4- and 6-positions of the phenol. Chemical substituents in *ortho*- and *para*-

position to the phenolic function are known to enhance the stability of phenoxyl radicals.[18] By analogy to the other pyridylphenol from Scheme 1 PhOH-CH_2-py is oxidized at much less positive potential than the PhOH reference molecule; in this specific case the potential difference amounts to ~0.6 V (Table 1).

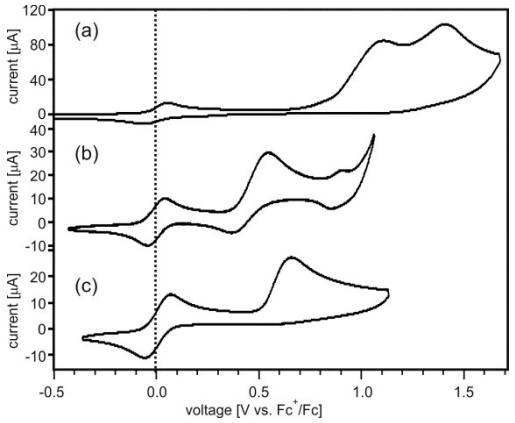

Figure 2. Cyclic voltammograms of the hydrogen-bonded phenols from Scheme 1 in dry CH_2Cl_2 in presence of 0.1 M $TBAPF_6$. (a) ^{t}Bu$_2$PhOH; (b) ^{t}Bu$_2$PhOH-CH_2-py; (c) PhOH-CH_2-py. The reversible waves at 0.0 V vs. Fc^+/Fc are due to ferrocene which was added in small quantities for internal voltage calibration; the scan rate was 100 mV/s

Table 1. Electrochemical potentials (*E*) for oxidation of the four phenol molecules and for reduction of the photoexcited [Re(phen)$(CO)_3$(py)]$^+$ complex.

redox couple	*E* [V vs. Fc^+/Fc]
$PhOH^+$/PhOH	1.25 [a] [d]
PhOH-CH_2-py^+/PhOH-CH_2-py	0.66 [b]
^{t}Bu$_2$$PhOH^+$/^{t}Bu$_2$PhOH	0.97 [b]
^{t}Bu$_2$PhOH-CH_2-py^+/^{t}Bu$_2$PhOH-CH_2-py	0.54 [b]
*[Re(phen)$(CO)_3$(py)]$^+$/[Re(phen)$(CO)_3$(py)]	0.77 [c] [d]

[a] From reference [15], converted from V vs. SCE to V vs. Fc^+/Fc by subtracting 0.38 V as described in ref. [16]; [b] Measured in this work, peak potentials from Figure 2, 0.1 M $TBAPF_6$ electrolyte in CH_2Cl_2; [c] from reference [6f]; [d] in CH_3CN. The previously reported value for ^{t}Bu$_2$PhOH-CH_2-py is 0.44 V vs. Fc^+/Fc in CH_3CN.[5f] The potential of ^{t}Bu$_2$PhOH is in line with the value reported in ref. [17] (0.519 V vs. NHE, addition of 0.624 V (according to ref. [16]) gives 1.14 V vs. Fc^+/Fc).

The electrochemistry of the [Re(phen)$(CO)_3$(py)]$^+$ complex and related rhenium(I) tricarbonyl diimines was explored extensively in the past.[7, 19] In Table 1 we merely give the electrochemical potential for one-electron reduction of ^{3}MLCT-excited [Re(phen)$(CO)_3$(py)]$^+$ as reported in the literature.[6f]

Optical absorption

Figure 3 shows UV-vis spectra of the four phenols and the rhenium(I) complex from Scheme 1 in CH_2Cl_2 at 25 °C. The important message from Figure 3 is that all four phenols are spectroscopically innocent at wavelengths longer than 330 nm. Between 270 and 280 nm they exhibit weak absorptions as previously reported for other phenols; in presence of covalently attached pyridine units the extinction between 270 nm and 280 nm increases because pyridine has itself weakly absorbing n-π* transitions occurring in this spectral range.[20] As reported previously, the [Re(phen)$(CO)_3$(py)]$^+$ complex exhibits a metal-to-ligand charge transfer (MLCT) band with maxima at 380 nm and 336 nm, while the absorption maximum at 276 nm has been attributed to phenanthroline-based electronic transitions.[19a, 19b] The most important observation from Figure 3 is that with light of 410 nm wavelength we can selectively excite the [Re(phen)$(CO)_3$(py)]$^+$ complex even in presence of large excess of any of the four phenols. Furthermore, there is no phenol absorption in the spectral range in which the rhenium(I) complex emits (450 nm – 700 nm); this is why in Figure 3 we show the entire spectral range between 250 nm and 700 nm. We note that phenol has a triplet energy (E_T) of 3.55 eV,[21] while the [Re(phen)$(CO)_3$(py)]$^+$ complex has $E_T \approx 2.75$ eV,[7, 19a] hence we can a priori rule out the possibility of ^{3}MLCT excited-state quenching by triplet-triplet energy transfer from [Re(phen)$(CO)_3$(py)]$^+$ to the phenols.[22]

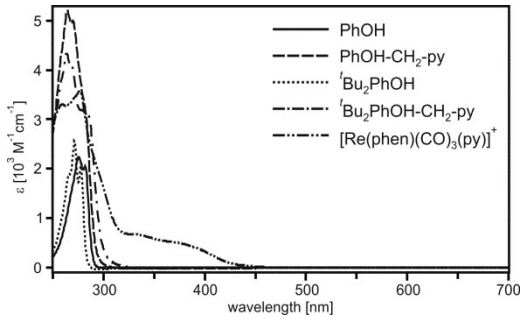

Figure 3. Optical absorption spectra of the four phenols and the rhenium(I) complex from Scheme 1.

Luminescence quenching experiments

The solid trace in Figure 4a is the emission spectrum of [Re(phen)$(CO)_3$(py)]$^+$ in aerated CH_2Cl_2 with 100 mM CH_3OH at 25 °C. The excitation wavelength was set at 410 nm. The broad and unstructured luminescence band is due to the typical ^{3}MLCT emission of rhenium(I) tricarbonyl diimines.[19a] The solid trace in Figure 4b shows the temporal evolution of the ^{3}MLCT luminescence from Figure 4a after excitation with ~10 ns laser pulses at 410 nm; detection occurred at 530 nm. The luminescence intensity decays in a single-exponential manner over more than two orders of magnitude and one extracts a ^{3}MLCT lifetime of 1.2 µs, in line with previous reports.[19a, 19b] The dashed lines in Figure 4a/4b were recorded in presence of variable concentrations (1 mM – 10 mM) of PhOH. No significant luminescence quenching is observed with PhOH, neither in intensity (Figure 4a) nor in decay time (Figure 4b). Likewise, when using deuterated phenol (PhOD), the emission intensity stays virtually unchanged (Figure 4c) and the luminescence decays are no faster than in the absence of PhOD (Figure 4d). We conclude that the ordinary phenol is unable to quench the ^{3}MLCT excited state of [Re(phen)$(CO)_3$(py)]$^+$ under the experimental conditions chosen here.

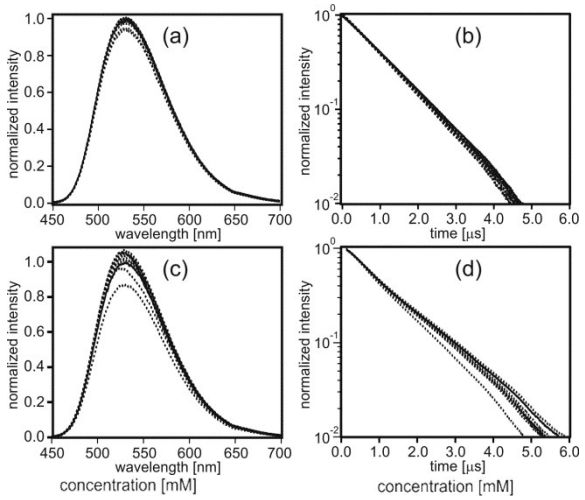

Figure 4. (a) Luminescence of $[Re(phen)(CO)_3(py)]^+$ in aerated CH_2Cl_2 with 100 mM CH_3OH in absence (solid line) and presence of increasing amounts of PhOH (dotted lines; 1 mM – 10 mM) after excitation at 410 nm; (b) luminescence decays of $[Re(phen)(CO)_3(py)]^+$ in the same solvent in absence (solid line) and presence of increasing amounts of PhOH (dotted lines) after excitation at 410 nm with laser pulses of ~10 ns width (detection wavelength: 530 nm); (c) same experiment as in (a) but with deuterated phenol (PhOD); (d) same experiment as in (b) but with deuterated phenol (PhOD). All y-axes are in arbitrary units; the intensity of the unquenched emission in (a) and (c) is normalized arbitrarily to 1; the intensity at t = 0 in (b) and (d) is normalized arbitrarily to 1.

Figure 5 shows the results of an analogous series of experiments performed with PhOH-CH_2-py. From Figure 5a we learn that the emission intensity of $[Re(phen)(CO)_3(py)]^+$ is significantly quenched in the presence of 1 mM to 10 mM PhOH-CH_2-py (dotted traces compared to solid trace). Similarly, the luminescence decays are strongly dependent on the PhOH-CH_2-py concentration (Figure 5b). When using deuterated PhOD-CH_2-py the luminescence decays (Figure 5d) are noticeably slower than for undeuterated PhOH-CH_2-py at equal concentration (Figure 5b). Likewise, in the luminescence intensity data of Figure 5c quenching at a given phenol concentration is noticeably weaker than for the undeuterated quencher in Figure 5a. Thus, there appears to be a significant H/D kinetic isotope effect (KIE).

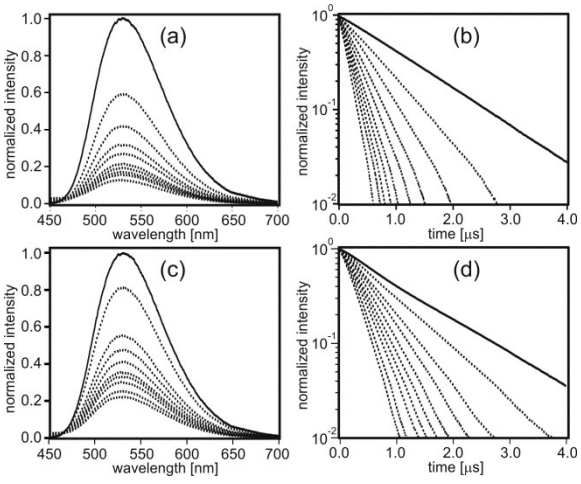

Figure 5. (a) Luminescence of $[Re(phen)(CO)_3(py)]^+$ in aerated CH_2Cl_2 with 100 mM CH_3OH in absence (solid line) and presence of increasing amounts of PhOH-CH_2-py (dotted lines; 1 mM – 10 mM) after excitation at 410 nm; (b) luminescence decays of $[Re(phen)(CO)_3(py)]^+$ in the same solvent in absence (solid line) and presence of increasing amounts of PhOH-CH_2-py (dotted lines) after excitation at 410 nm with laser pulses of ~10 ns width (detection wavelength: 530 nm); (c) same experiment as in (a) but with deuterated phenol (PhOD-CH_2-py) and 100 mM CH_3OD; (d) same experiment as in (b) but with deuterated phenol (PhOD-CH_2-py) and 100 mM CH_3OD. All y-axes are in arbitrary units; the intensity of the unquenched emission in (a) and (c) is normalized arbitrarily to 1; the intensity at t = 0 in (b) and (d) is normalized arbitrarily to 1.

Figure 6a is a Stern-Volmer plot based on the luminescence *intensity* data from Figures 4/5, and Figure 6b is a Stern-Volmer plot based on the luminescence *lifetime* data from Figures 4/5.[23] The open circles in Figure 6a/6b represent data obtained using PhOH-CH_2-py, the open squares represent data obtained using the deuterated analogue PhOD-CH_2-py. Linear regression fits yield the Stern-Volmer constants (K_{SV}) given in the third (ordinary phenols) and fourth column (deuterated phenols) of Table 2.

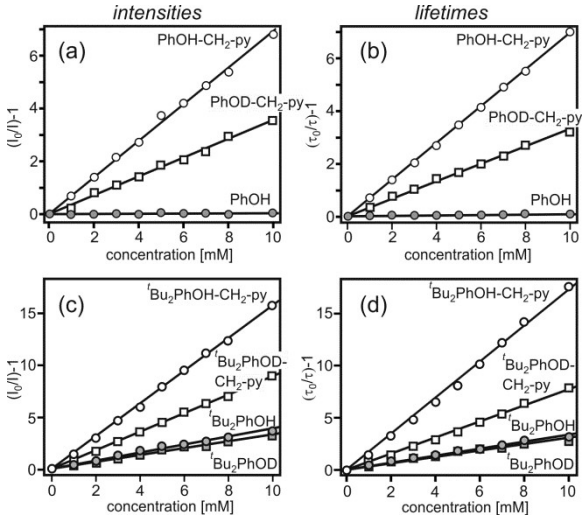

Figure 6. (a) Stern-Volmer plot based on the luminescence *intensity* data from Figures 4/5; open circles: PhOH-CH_2-py, open squares: PhOD-CH_2-py, grey filled circles: PhOH. (b) Stern-Volmer plot based on the luminescence *lifetime* data from Figures 4/5; open circles: PhOH-CH_2-py, open squares: PhOD-CH_2-py, grey filled circles: PhOH. (c) Stern-Volmer plot based on the luminescence *intensity* data from Figures S1/S2; open circles: ^{t}Bu$_2$PhOH-CH_2-py, open squares: ^{t}Bu$_2$PhOD-CH_2-py, grey filled circles: ^{t}Bu$_2$PhOH, grey filled squares: ^{t}Bu$_2$PhOD. (d) Stern-Volmer plot based on the luminescence *lifetime* data from Figures S1/S2; open circles: ^{t}Bu$_2$PhOH-CH_2-py, open squares: ^{t}Bu$_2$PhOD-CH_2-py, grey filled circles: ^{t}Bu$_2$PhOH, grey filled squares: ^{t}Bu$_2$PhOD.

The H/D KIE mentioned above shows up directly in the Stern-Volmer constants: From the intensity data in Figure 6 one extracts $K_{SV,\,H}$ = 691±7 M^{-1} (for PhOH-CH_2-py) and $K_{SV,\,D}$ = 355±5 M^{-1} (for PhOD-CH_2-py), the lifetime data in Figure 6b yield $K_{SV,\,H}$ = 701±3 M^{-1} (for PhOH-CH_2-py) and $K_{SV,\,D}$ = 334±6 M^{-1} (for PhOD-CH_2-py). Based on the ^{3}MLCT lifetime of $[Re(phen)(CO)_3(py)]^+$ (1.2 µs in aerated CH_2Cl_2, see above) we calculate rate constants for bimolecular excited-state quenching of $k_{Q,\,H} = (5.9\pm0.1)\cdot10^8$ M^{-1} s^{-1} for PhOH-CH_2-py and $k_{Q,\,D} = (2.8\pm0.1)\cdot10^8$ M^{-1} s^{-1} for PhOD-CH_2-py (fifth and sixth column of Table 2).[23] The H/D KIE is the ratio between $k_{Q,\,H}$ and $k_{Q,\,D}$ and amounts to 2.1±0.1 (last column of Table 2).[6g] From the luminescence intensity data in Figure 6a one extracts $k_{Q,\,H} = (5.9\pm0.1)\cdot10^8$ M^{-1} s^{-1} for PhOH-CH_2-py and $k_{Q,\,D} = (3.0\pm0.1)\cdot10^8$ M^{-1} s^{-1} for PhOD-CH_2-py, yielding a value of KIE (2.0±0.1) in accordance with the lifetime data.

Table 2. Results from luminescence quenching experiments

phenol	Exp. type	$K_{SV,H}$ [M^{-1}]	$K_{SV,D}$ [M^{-1}]	$k_{Q,H}$ [$M^{-1}.s^{-1}$]	$k_{Q,D}$ [$M^{-1}.s^{-1}$]	KIE
PhOH/D	intensity	3.4±1.2	0.5±3.7	$(2.9±1.0)\cdot10^6$	$(0.4±3.1)\cdot10^6$	N/A
	lifetime	8.4±0.4	13.8±1.0	$(7.1±0.3)\cdot10^6$	$(11.7±0.8)\cdot10^6$	N/A
PhOH/D-CH_2-py	intensity	691±7	355±5	$(5.9±0.1)\cdot10^8$	$(3.0±0.1)\cdot10^8$	2.0±0.1
	lifetime	701±3	334±6	$(5.9±0.1)\cdot10^8$	$(2.8±0.1)\cdot10^8$	2.1±0.1
^{t}Bu$_2$PhOH/D	intensity	391±8	332±8	$(3.3±0.1)\cdot10^8$	$(2.8±0.1)\cdot10^8$	1.2±0.1
	lifetime	437±11	309±10	$(3.7±0.1)\cdot10^8$	$(2.6±0.1)\cdot10^8$	1.4±0.1
^{t}Bu$_2$PhOH/D-CH_2-py	intensity	1572±9	892±5	$(13.3±0.1)\cdot10^8$	$(7.6±0.1)\cdot10^8$	1.8±0.1
	lifetime	1648±8	773±8	$(14.0±0.1)\cdot10^8$	$(6.6±0.1)\cdot10^8$	2.1±0.1

Stern-Volmer constants obtained from emission intensity or lifetime experiments with normal ($K_{SV,H}$) and deuterated phenols ($K_{SV,D}$). Rate constants for bimolecular excited-state quenching with normal ($k_{Q,H}$) and deuterated phenols ($k_{Q,D}$); calculated from $K_{SV,H}$ and $K_{SV,D}$ values using the lifetime of ^{3}MLCT-excited [Re(phen)(CO)$_3$(py)]$^+$ in aerated CH_2Cl_2 with 100 mM CH_3OH (1177 ns). H/D kinetic isotope effect (KIE) calculated from the ratio of $k_{Q,H}$ and $k_{Q,D}$

The grey filled circles in Figures 6a/6b represent data obtained for the undeuterated reference phenol PhOH. One extracts $K_{SV,H}$ = 3.4±1.2 M^{-1} from the intensity data in Figure 6a and $K_{SV,H}$ = 8.4±0.4 M^{-1} from the lifetime data in Figure 6b, which in turn yields $k_{Q,H}$ values on the order of 10^6 $M^{-1}s^{-1}$. This order of magnitude of $k_{Q,H}$ underscores what in principle is already evident from the raw data in Figure 4: Reductive excited-state quenching by PhOH is not kinetically competitive with other (radiative and nonradiative) deactivation processes of photoexcited [Re(phen)(CO)$_3$(py)]$^+$. Thus, even though $k_{Q,D}$ values for deuterated phenol are technically available from the data in Figures 4c/4d, calculation of an H/D KIE is not meaningful in the case of the simple reference phenol.

Figures 6c/6d show Stern-Volmer plots based on [Re(phen)(CO)$_3$(py)]$^+$ luminescence quenching experiments with ^{t}Bu$_2$PhOH (grey filled circles), ^{t}Bu$_2$PhOD (grey filled squares), ^{t}Bu$_2$PhOH-CH_2-py (open circles), and ^{t}Bu$_2$PhOD-CH_2-py (open squares). The respective raw data are shown in Figures S1 and S2 of the Supporting Information. The bimolecular rate constants for excited-state quenching with ^{t}Bu$_2$PhOH and its deuterated congener extracted from this data are all around $3\cdot10^8$ M^{-1} s^{-1} (Table 2), for ^{t}Bu$_2$PhOH/D-CH_2-py the k_Q-values are about a factor of 3 larger. H/D KIEs range from close to 1.0 for ^{t}Bu$_2$PhOH to ~2.0 for ^{t}Bu$_2$PhOH-CH_2-py.

All luminescence quenching experiments were performed in presence of 100 mM CH_3OH / CD_3OD to ensure deuteration of the phenol molecules for the KIE studies. Use of pure CH_2Cl_2 or CD_2Cl_2 leads to markedly lower KIEs, presumably due to D/H exchange of the deuterated phenols when brought into contact with glassware / cuvettes.

Figure 7 shows a plot of the (average) k_Q values versus standard Gibbs free energy of reaction (ΔG_{ET}^{0*}) associated with electron transfer from the individual phenols to ^{3}MLCT-excited [Re(phen)(CO)$_3$(py)]$^+$. The free energies were calculated based on the redox potentials from Table 1, using the previously determined electrochemical potential for one-electron reduction of photoexcited [Re(phen)(CO)$_3$(py)]$^+$ of 0.77 V vs. Fc^+/Fc (bottom row of Table 1).[6f]

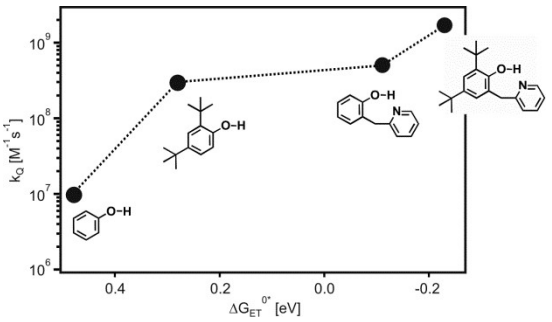

Figure 7. Rate constant ($k_{Q,H}$; from Table 2) for ^{3}MLCT excited-state quenching of [Re(phen)(CO)$_3$(py)]$^+$ versus driving-force for reductive excited-state quenching (ΔG_{ET}^{0*}; estimated on the basis of the data in Table 1).

Transient absorption

Figure 8a shows the transient absorption spectrum obtained from an acetonitrile solution with $6.7\cdot10^{-5}$ M [Re(phen)(CO)$_3$(py)]$^+$ and 10 mM ^{t}Bu$_2$PhOH-CH_2-py. Selective excitation of the rhenium(I) complex occurred at 355 nm (Figure 2) with laser pulses of ~10 ns width. The data was time-averaged in a window ranging from 0 to 200 ns after the excitation pulse. The spectrum in Figure 8a exhibits the signatures of the reduced rhenium tricarbonyl diimine complex and neutral phenoxyl radical at the same time. The intense narrow band centered around 315 nm and the weaker featureless band extending from ~340 nm to nearly 550 nm is typical for the one-electron reduced form of the rhenium complex considered here.[6e, 24] On the other hand, the narrow peaks at 390 nm and 409 nm (dashed vertical arrows) are due to the phenoxyl radical as becomes evident from comparison to the spectrum in Figure 8b. The latter spectrum was recorded after 355-nm excitation of a CH_3CN solution containing 2 mM ^{t}Bu$_2$PhOH-CH_2-py, 5 mM 1,4-dicyanonaphthalene, and 0.3 M biphenyl. These reaction conditions (making use of 1,4-dicyanonaphthalene as a photosensitizer and biphenyl as a co-donor) represent an efficient means for the photogeneration of neutral phenoxyl radicals.[25] In presence of phenol the spectral signatures of reduced 1,4-dicyanonaphthalene and oxidized biphenyl have disappeared within 6 μs, and hence when detecting with a delay of 6.6 μs after the 10-ns laser pulse one obtains the spectrum shown in Figure 8b, representing the

absorption spectrum of the phenoxyl radical of ^{t}Bu$_2$PhOH-CH$_2$-py.[25-26] The observation of the same spectral features in Figure 8a is direct evidence for a PCET reaction, since one detects the oxidized and deprotonated form of the phenol in addition to the reduced form of the rhenium(I) reaction partner. The proton acceptor site is most likely the pyridine unit of ^{t}Bu$_2$PhOH-CH$_2$-py but this cannot be monitored by transient absorption spectroscopy.

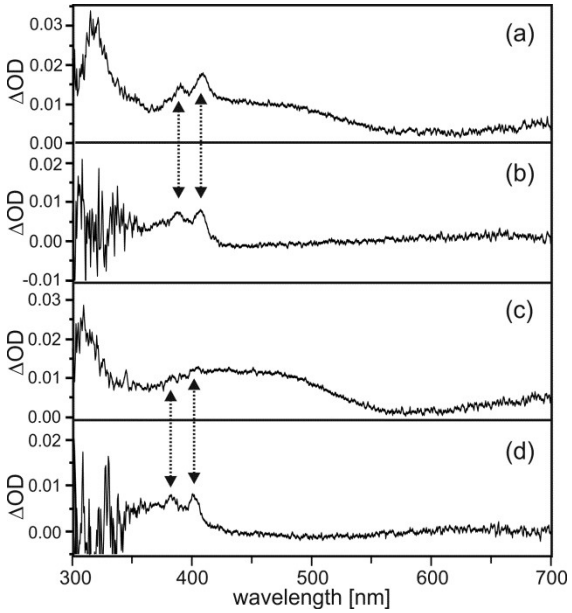

Figure 8. Transient absorption spectra measured in a time window ranging from 0 to 200 ns after excitation with 10-ns laser pulses at 355 nm. (a) $6.7 \cdot 10^{-5}$ M CH_3CN solution of $[Re(phen)(CO)_3(py)]^+$ with 10 mM ^{t}Bu$_2$PhOH-CH$_2$-py; (b) 2 mM CH_3CN solution of ^{t}Bu$_2$PhOH-CH$_2$-py with 5 mM 1,4-dicyanonaphthalene and 0.3 M biphenyl; this set of data was detected with a time delay of 6.6 μs after the excitation pulses. (c) $6.7 \cdot 10^{-5}$ M CH_3CN solution of $[Re(phen)(CO)_3(py)]^+$ with 19.6 mM PhOH-CH$_2$-py; (d) 2.1 mM CH_3CN solution of PhOH-CH$_2$-py with 5 mM 1,4-dicyanonaphthalene and 0.3 M biphenyl; this set of data was detected with a time delay of 6.6 μs after the excitation pulses.

Figure 8c and 8d show data from experiments which are analogous to those in Figures 8a and 8b but using solutions with PhOH-CH$_2$-py instead of ^{t}Bu$_2$PhOH-CH$_2$-py. Qualitatively similar transient absorption spectra are obtained, but the phenoxyl radical signals are markedly weaker for PhOH-CH$_2$-py than for ^{t}Bu$_2$PhOH-CH$_2$-py. However, careful inspection of the data in Figure 8c reveals that the respective signals, observed at 382 nm and 402 nm in Figure 8d, are indeed detectable in the rhenium / PhOH-CH$_2$-py mixture (dashed vertical arrows). We note that phenoxyl radicals typically have extinction coefficients on the order of 3000 l·mol^{-1}·cm^{-1},[26] hence the weakness of some of the signals in Figure 8 is not particularly unusual. At any rate the data provides direct evidence for PCET photoproducts in both rhenium(I) / pyridylphenol reaction couples.

Conclusion

The hydrogen-bonded pyridylphenols from Scheme 1 quench the ^{3}MLCT excited-state of $[Re(phen)(CO)_3(py)]^+$ at significantly higher rates than ordinary reference phenols. This observation is in line with the substantially lower oxidation potentials (~0.5 V) of the pyridylphenols relative to the reference phenols. The lower oxidation potentials in turn are the result of proton-coupled oxidation processes, as demonstrated in prior studies.[2e, 5d, 5n] Thus we conclude that in the PhOH-CH$_2$-py / rhenium(I) and ^{t}Bu$_2$PhOH-CH$_2$-py / rhenium(I) reaction couples considered here the overall quenching process is a CPET reaction involving electron transfer from the phenols to the photoexcited metal complex and transfer of the phenolic proton to the pyridine base. Transient absorption data support this conclusion because they provide direct evidence for the photogeneration of neutral phenoxyl radicals. H/D kinetic isotope effects on the order of 2 point to the involvement of concerted proton-electron transfer in the excited-state chemistry, in line with the prior notion that the oxidation potentials of the pyridylphenols can only be that much lower than those of ordinary phenols (~0.5 V) because electron release is inherently coupled to deprotonation.[2e, 5d, 5n]

Interestingly, excited-state quenching with ^{t}Bu$_2$PhOH by simple electron transfer is already quite efficient ($(3.3\pm0.1)\cdot10^8$ M^{-1} s^{-1}), yet ^{t}Bu$_2$PhOH-CH$_2$-py quenches the rhenium ^{3}MLCT state even more rapidly ($(13.3\pm0.1)\cdot10^8$ M^{-1} s^{-1}) and with an H/D KIE of ~2, suggesting that CPET stays kinetically highly competitive with an electron transfer / proton transfer sequence even in a situation in which the initial electron transfer step is thermodynamically possible

Experimental Section

A suspension of NaH (60% in mineral oil, 1.20 g, 30 mmol) in anhydrous THF (6 ml) was cooled to 0°C and a solution of 2-bromophenol (**1**) (3.44 g, 20 mmol) in anhydrous THF (8 ml) was added dropwise over 1 hour under N_2 atmosphere. After stirring for an additional 10 minutes iodomethane (9.2 g, 64.8 mmol) was added, and the mixture was allowed to warm up to room temperature prior to refluxing for 19 hours. After cooling back to room temperature water was added (160 ml), and the product was extracted with pentane (3 × 100 ml). The combined organic phases were dried over anhydrous $MgSO_4$, and the solvent was removed on a rotary evaporator. Subsequent purification on silica gel with CH_2Cl_2 as an eluent ($R_f \approx 0.3$) gave 1-bromo-2-methoxybenzene (**2**) in 97% yield.[27] ^{1}H NMR (300 MHz, $CDCl_3$): δ (ppm) = 3.89 (s, 3 H), 6.78-6.95 (m, 2 H), 7.27 (td, *J* = 8.2, 6.1 Hz, 1 H), 7.54 (dd, *J* = 7.8, 1.6 Hz, 1 H).

The same procedure using identical molar quantities of starting materials was employed for the synthesis of 1-bromo-3,5-di-*tert*-butyl-2-methoxybenzene (**4**) from 2-bromo-4,6-di-*tert*-butylphenol (**3**). On silica gel using CH_2Cl_2 as an eluent, product **4** has $R_f \approx 0.6$, the yield was 97%. ^{1}H NMR (300 MHz, $CDCl_3$): δ (ppm) = 1.30 (s, 9 H), 1.40 (s, 9 H), 3.91 (s, 3 H), 7.28 (d, *J* = 2.4 Hz, 1 H), 7.41 (d, *J* = 2.4 Hz, 1 H).

For the synthesis of molecule **5** a solution of 2-picoline (200 mmol) in anhydrous THF (200 ml) was cooled to -30°C and 1.6 M *n*-butyllithium in hexane (200 mmol) was added slowly. After stirring at this temperature for 30 minutes diisopropyl ketone was added slowly, and the reaction mixture was stirred for another 2 hours at room temperature. Subsequently water (300 ml) was added and the resulting mixture was extracted with ethyl acetate (3 × 200 ml). The combined organic phases were dried over anhydrous $MgSO_4$, and the solvent was removed using a rotary evaporator. The raw product was purified by column chromatography on silica gel using a 3:1 (v:v) mixture of pentane and ethyl acetate as an eluent ($R_f \approx 0.6$). This procedure afforded pure molecule **5** in 83% yield.[8] ^{1}H NMR (300 MHz, $CDCl_3$): δ (ppm) = 0.88 (dd, *J* = 6.9, 4.9 Hz, 12 H), 1.90 (m, 2 H), 2.98 (s, 2 H), 6.29 (s, 1 H), 7.08-7.13 (m, 1 H), 7.15 (d, *J* = 7.8 Hz, 1 H), 7.58 (td, *J* = 7.7, 1.9 Hz, 1 H), 8.43 (ddd, *J* = 4.9, 1.8, 0.9 Hz, 1 H).

Using a heat gun Cs_2CO_3 (27.90 g, 85.6 mmol) was dried under vacuum. Subsequently, palladium trifluoroacetate (1.18 g, 3.6 mmol), tricyclohexylphosphine (2.00 g, 7.1 mmol), dry *p*-xylene (150 ml), 1-bromo-2-methoxybenzene (**2**) (16.00 g, 85.6 mmol), and pyridine **5**

(14.70 g, 71.3 mmol) were added under nitrogen. The reaction mixture was refluxed under N_2 overnight. After cooling to room temperature the mixture was filtered, and the solvent was evaporated under reduced pressure. Column chromatography on silica gel using a 5:1 (v:v) mixture of pentane and ethyl acetate ($R_f \approx 0.1$) afforded the coupling product **6** as a yellow liquid in 73% yield.[8] ^{1}H NMR (300 MHz, $CDCl_3$): δ (ppm) = 3.80 (s, 3 H), 4.17 (s, 2 H), 6.90 (ddd, *J* = 8.1, 6.3, 2.6 Hz, 2 H), 7.03-7.14 (m, 2 H), 7.14-7.26 (m, 2 H), 7.54 (td, *J* = 7.7, 1.9 Hz, 1 H), 8.49-8.58 (m, 1 H).

Molecule **6** (0.15 g, 0.78 mmol) was dissolved in aqueous HBr (47%, 4 ml) and the mixture was refluxed for 19 hours.[9] After evaporation of excess acid, water was added to the solid residue, and the solution was neutralized by addition of an aqueous K_2CO_3 solution. The product (**7**) was extracted with CH_2Cl_2, and the combined organic phases were dried over anhydrous $MgSO_4$ prior to solvent removal on a rotary evaporator. The raw product was purified by column chromatography on silica gel using CH_2Cl_2 as an eluent ($R_f \approx 0.4$) affording product **7** (PhOH-CH_2-py) as a white solid in 57% yield. ^{1}H NMR (300 MHz, $CDCl_3$): δ (ppm) = 4.10 (s, 2 H), 6.82 (td, *J* = 7.4, 1.3 Hz, 1 H), 6.95-7.02 (m, 1 H), 7.13-7.21 (m, 3 H), 7.32 (d, *J* = 7.8 Hz, 1 H), 7.69 (td, *J* = 7.7, 1.8 Hz, 1 H), 8.46 (ddd, *J* = 5.0, 1.8, 0.8 Hz, 1 H), 11.67 (s, 1 H). ^{13}C NMR (75 MHz, $CDCl_3$): δ (ppm) = 41.7, 118.5, 119.9, 121.9, 122.8, 126.2, 128.7, 130.2, 138.2, 147.8, 156.7, 161.0. MS (EI) (m/z) = 186.0921 ([M+H]$^+$, calc.: 186.0913). Anal. calcd. for $C_{13}H_{13}NO$ (%): C: 77.81, H: 5.99, N: 7.56; found: C: 77.63, H: 5.97, N: 7.47.

For the synthesis of molecule **8** from 1-bromo-3,5-di-*tert*-butyl-2-methoxybenzene (**4**) and pyridine **5** the same procedure as described above for molecule **6** was used.[8] The quantities of reactants used in this case were as follows: Cs_2CO_3: 22.81 g, 70.0 mmol; palladium trifluoroacetate: 0.97 g, 2.9 mmol; tricyclohexylphosphine: 1.63 g, 5.8 mmol; dry *p*-xylene: 150 ml; 1-bromo-3,5-di-*tert*-butyl-2-methoxybenzene (**4**): 20.86 g, 70 mmol; pyridine **5**: 12.10 g, 58.3 mmol. Using the same chromatography conditions as described above for molecule **6**, the R_f value is ~0.3, and molecule **8** was obtained in 69% yield as a yellow oil. ^{1}H NMR (300 MHz, $CDCl_3$): δ (ppm) = 1.26 (s, 9 H), 1.43 (s, 9 H), 3.75 (s, 3 H), 4.27 (s, 2 H), 6.98-7.17 (m, 3 H), 7.26-7.31 (m, 1 H), 7.56 (td, *J* = 7.7, 1.9 Hz, 1 H), 8.57 (ddd, *J* = 4.9, 1.8, 0.9 Hz, 1 H).

When subjecting molecule **8** to the same methoxyl-deprotection reaction with aqueous HBr as described above for molecule **6**, not only the methoxyl-group but also the *tert.*-butyl substituents of molecule **8** were cleaved off and the reaction afforded molecule **7**. It was therefore necessary to apply the following procedure in order to obtain molecule **9**:[10] To a suspension of NaH (60% in mineral oil, 0.31 g, 12.8 mmol) in dry *N,N*-dimethylformamide under N_2 atmosphere ethanethiol (0.69 g, 11.2 mmol) was added dropwise. Then molecule **8** (0.50 g, 1.6 mmol) was added and the reaction mixture was stirred at 100 °C overnight. After cooling to room temperature, H_2O (4 ml), 1 M aqueous HCl (13 ml) and phosphate buffer (0.5 M, pH = 7) were added, and the mixture was extracted with diethyl ether (3 × 50 ml). The combined organic phases were dried over anhydrous $MgSO_4$, and the solvent was removed on a rotary evaporator. Purification by three successive chromatography columns on silica gel using a 7:3 (v:v) pentane/dichloromethane mixture ($R_f \approx 0.5$) gave product **9** (^{t}Bu$_2$PhOH-CH_2-py) in 65% yield as a white solid. ^{1}H NMR (300 MHz, $CDCl_3$): δ (ppm) = 1.31 (s, 9 H), 1.47 (s, 9 H), 4.10 (s, 2 H), 7.06 (d, *J* = 2.5 Hz, 1 H), 7.17 (ddd, *J* = 7.6, 5.0, 1.1 Hz, 1 H), 7.24 (d, *J* = 2.4 Hz, 1 H), 7.34 (d, *J* = 7.8 Hz, 1 H), 7.67 (td, *J* = 7.7, 1.8 Hz, 1 H), 8.45 (ddd, *J* = 5.0, 1.7, 0.9 Hz, 1 H), 11.40 (s, 1 H). ^{13}C NMR (75 MHz, $CDCl_3$): δ (ppm) = 28.8, 30.7, 33.2, 34.1, 41.2, 120.7, 121.7, 122.0, 123.9, 125.3, 136.9, 137.0, 140.4, 146.6, 151.8, 160.5. MS (EI) (m/z) = 298.2168 ([M+H]$^+$, calc.: 298.2165). Anal. calcd. for $C_{20}H_{27}NO{\cdot}0.1C_2H_6NO{\cdot}0.5C_5H_{12}$ (%): C: 80.35, H: 9.97, N: 4.52; found: C: 80.29, H: 10.02, N: 4.63.

Deuteration of the phenolic functions occurred by dissolving the individual phenol molecules in a 1:1 mixture of CH_3CN and D_2O (99.9%) followed by subsequent solvent removal on a rotary evaporator; this procedure was accomplished twice in order to ensure high isotope purity. Luminescence quenching experiments in CH_2Cl_2 occurred in presence of 100 mM CD_3OD (99.99%) in order to avoid significant D/H exchange through contact of the phenols with glassware and cuvettes. For experiments with undeuterated phenols, 100 mM CH_3OH was added.

The $[Re(phen)(CO)_3(py)]^+$ complex was available from prior studies in the form of its hexafluorophosphate salt.[6e, 6f]

^{1}H and ^{13}C NMR spectra were measured on a Bruker B-ACS-120 instrument. Electron-impact mass spectrometry was made with a Finnigan MAT 95 spectrometer. Elemental analyses were performed with a Vario EL3 instrument. For cyclic voltammetry a Versastat3-200 potentiostat from Princeton Applied Research was used. A glassy carbon working electrode, a platinum counter electrode, and a silver quasi-reference electrode were employed. 0.1 M tetrabutylammonium hexafluorophosphate ($TBAPF_6$) was used as an electrolyte; prior to voltage sweeps at rates of 0.1 V/s the solvent was flushed with nitrogen. Optical absorption spectra were recorded on a Cary 5000 instrument from Varian, steady-state luminescence experiments were performed on a Fluorolog-3 apparatus from Horiba Jobin-Yvon. Luminescence lifetime experiments were performed in Geneva using a home-built setup comprised of a Quantel Brilliant Nd:YAG laser with an integrated magic prism OPO as an excitation source and a detection system consisting of a Spex 270M monochromator, an R928 photomultiplier from Hamamatsu, and a Tektronix TDS 540B digital oscilloscope. Transient absorption experiments were performed in Göttingen using an LP920-KS instrument from Edinburgh Instruments equipped with an iCCD camera from Andor and a Quantel Brilliant b laser as an excitation source.

For the X-ray structures crystals of **7** and **9** were grown by slow evaporation of the solvent at room temperature. They were selected and mounted with inert oil on a kapton MicroMount. The data of **7** were collected at 100 K on a Bruker Apex II Ultra with mirror optics. The data of **9** were collected on a Bruker smart Apex II Quazar with an Incoatec IμS.[28] Data reduction was performed with SAINT,[29] and an empirical absorption correction with SADABS[30] was applied. The structures were solved by direct methods (SHELXS-97)[31] and refined by full-matrix least-squares methods against F^2 with SHELXL-97[31] and the shelXle[32] GUI. All non-hydrogen atoms were refined with anisotropic displacement parameters. The hydrogen atoms were refined isotropically on calculated positions using a riding model with their U_{iso} values constrained to 1.5 times the U_{eq} of their pivot atoms for terminal sp^3 carbon atoms and 1.2 times for all other carbon atoms. Crystallographic data (excluding structure factors) for the structures reported in this paper have been deposited with the Cambridge Crystallographic Data Centre. The CCDC numbers, crystal data and experimental details for the X-ray measurements are listed in the supporting information. CCDC 887369 (**7**) and 887370 (**9**) contain the supplementary crystallographic data for this paper. These data can be obtained free of charge from The Cambridge Crystallographic Data Centre via www.ccdc.cam.ac.uk/data_request/cif.

Acknowledgements

This research was supported by the Swiss National Science Foundation (SNSF) through grant number PP002-110611, by the Danish National Research Foundation (DNRF) funded Center for Materials Crystallography (CMC), and by the Deutsche Forschungsgemeinschaft (DFG) through IRTG-1422 and through grant number INST186/872-1. The MWK Niedersachsen is thanked for co-funding the transient absorption spectrometer. J. M. Mayer and T. F. Markle are acknowledged for valuable discussions.

Keywords: Electron transfer; proton transfer; photochemistry transient absorption; luminescence

[1] a) I. Bertini, H. B. Gray, E. I. Stiefel, J. S. Valentine, *Biological Inorganic Chemistry*, University Science Books, Sausalito, California, **2007**; b) G. Renger, T. Renger, *Photosynth. Res.* **2008**, *98*, 53-80.

[2] a) B. A. Barry, G. T. Babcock, *Proc. Natl. Acad. Sci. U. S. A.* **1987**, *84*, 7099-7103; b) S. Y. Reece, D. G. Nocera, *Annu. Rev. Biochem.* **2009**, *78*, 673-699; c) T. J. Meyer, M. H. V. Huynh, H. H. Thorp, *Angew. Chem. Int. Ed.* **2007**, *46*, 5284-5304; d) M. H. V. Huynh, T. J. Meyer, *Chem. Rev.* **2007**, *107*, 5004-5064; e) J. M. Mayer, I. J. Rhile, F. B. Larsen, E. A. Mader, T. F. Markle, A. G. DiPasquale, *Photosynth. Res.* **2006**, *87*, 3-20; f) J. L. Dempsey, J. R. Winkler, H. B. Gray, *Chem. Rev.* **2010**, *110*, 7024-7039; g) S. Hammes-Schiffer, A. A. Stuchebrukhov, *Chem. Rev.* **2010**, *110*, 6939-6960; h) J. J. Warren, J. R. Winkler, H. B. Gray, *FEBS Lett.* **2012**, *586*, 596-602.

[3] a) L. Benisvy, R. Bittl, E. Bothe, C. D. Garner, J. McMaster, S. Ross, C. Teutloff, F. Neese, *Angew. Chem. Int. Ed.* **2005**, *44*, 5314-5317; b) T. Maki, Y. Araki, Y. Ishida, O. Onomura, Y. Matsumura, *J. Am. Chem. Soc.* **2001**, *123*, 3371-3372; c) T. Lachaud, A. Quaranta, Y. Pellegrin, P. Dorlet, M. F. Charlot, S. Un, W. Leibl, A. Aukauloo, *Angew. Chem. Int. Ed.* **2005**, *44*, 1536-1540.

[4] a) C. Costentin, M. Robert, J.-M. Savéant, *Acc. Chem. Res.* **2010**, *43*, 1019-1029; b) C. Costentin, M. Robert, J. M. Savéant, *J. Am. Chem. Soc.* **2006**, *128*, 4552-4553; c) J. Bonin, C. Costentin, M. Robert, J. M. Savéant, *Org. Biomol. Chem.* **2011**, *9*, 4064-4069; d) C. Costentin, M. Robert, J. M. Savéant, C. Tard, *Phys. Chem. Chem. Phys.* **2011**, *13*, 5353-5358; e) J. Bonin, C. Costentin, C. Louault, M. Robert, M. Routier, J. M. Savéant, *Proc. Natl. Acad. Sci. U. S. A.* **2010**, *107*, 3367-3372; f) C. Costentin, M. Robert, J. M. Savéant, C. Tard, *Angew. Chem. Int. Ed.* **2010**, *49*, 3803-3806.

[5] a) G. F. Moore, M. Hambourger, M. Gervaldo, O. G. Poluektov, T. Rajh, D. Gust, T. A. Moore, A. L. Moore, *J. Am. Chem. Soc.* **2008**, *130*, 10466-10467; b) S. Y. Reece, D. G. Nocera, *J. Am. Chem. Soc.* **2005**, *127*, 9448-9458; c) I. J. Rhile, T. F. Markle, H. Nagao, A. G. DiPasquale, O. P. Lam, M. A. Lockwood, K. Rotter, J. M. Mayer, *J. Am. Chem. Soc.* **2006**, *128*, 6075-6088; d) I. J. Rhile, J. M. Mayer, *J. Am. Chem. Soc.* **2004**, *126*, 12718-12719; e) T. F. Markle, I. J. Rhile, A. G. DiPasquale, J. M. Mayer, *Proc. Natl. Acad. Sci. U. S. A.* **2008**, *105*, 8185-8190; f) T. F. Markle, J. M. Mayer, *Angew. Chem., Int. Ed.* **2008**, *47*, 738-740; g) A. Magnuson, M. Anderlund, O. Johansson, P. Lindblad, R. Lomoth, T. Polivka, S. Ott, K. Stensjö, S. Styring, V. Sundström, L. Hammarström, *Acc. Chem. Res.* **2009**, *42*, 1899-1909; h) O. Johansson, H. Wolpher, M. Borgström, L. Hammarström, J. Bergquist, L. C. Sun, B. Åkermark, *Chem. Commun.* **2004**, 194-195; i) L. Hammarström, S. Styring, *Energy Environ. Sci.* **2011**, *4*, 2379-2388; j) A. Magnuson, H. Berglund, P. Korall, L. Hammarström, B. Åkermark, S. Styring, L. C. Sun, *J. Am. Chem. Soc.* **1997**, *119*, 10720-10725; k) M. Sjödin, T. Irebo, J. E. Utas, J. Lind, G. Merenyi, B. Åkermark, L. Hammarström, *J. Am. Chem. Soc.* **2006**, *128*, 13076-13083; l) L. C. Sun, M. Burkitt, M. Tamm, M. K. Raymond, M. Abrahamsson, D. LeGourriérec, Y. Frapart, A. Magnuson, P. H. Kenéz, P. Brandt, A. Tran, L. Hammarström, S. Styring, B. Åkermark, *J. Am. Chem. Soc.* **1999**, *121*, 6834-6842; m) M.-T. Zhang, T. Irebo, O. Johansson, L. Hammarström, *J. Am. Chem. Soc.* **2011**, *133*, 13224-13227; n) T. F. Markle, I. J. Rhile, J. M. Mayer, *J. Am. Chem. Soc.* **2011**, *133*, 17341-17352.

[6] a) C. J. Gagliardi, B. C. Westlake, C. A. Kent, J. J. Paul, J. M. Papanikolas, T. J. Meyer, *Coord. Chem. Rev.* **2010**, *254*, 2459-2471; b) O. S. Wenger, *Chem.-Eur. J.* **2011**, *17*, 11692-11702; c) T. Irebo, S. Y. Reece, M. Sjödin, D. G. Nocera, L. Hammarström, *J. Am. Chem. Soc.* **2007**, *129*, 15462-15464; d) B. C. Westlake, M. K. Brennaman, J. J. Concepcion, J. J. Paul, S. E. Bettis, S. D. Hampton, S. A. Miller, N. V. Lebedeva, M. D. E. Forbes, A. M. Moran, T. J. Meyer, J. M. Papanikolas, *Proc. Natl. Acad. Sci. U. S. A.* **2011**, *108*, 8554-8558; e) T. I. A. Gerber, E. Hosten, P. Mayer, Z. R. Tshentu, *J. Coord. Chem.* **2006**, *59*, 243-253; f) J. F. Ireland, P. A. H. Wyatt, *Adv. Phys. Org. Chem.* **1976**, *12*, 131-160; g) C. Bronner, O. S. Wenger, *J. Phys. Chem. Lett.* **2012**, *3*, 70-74.

[7] W. B. Connick, A. J. Di Bilio, M. G. Hill, J. R. Winkler, H. B. Gray, *Inorg. Chim. Acta* **1995**, *240*, 169-173.

[8] T. Niwa, H. Yorimitsu, K. Oshima, *Angew. Chem. Int. Ed.* **2007**, *46*, 2643-2645.

[9] O. Mongin, P. Rocca, L. Thomas-dit-Dumont, F. Trécourt, F. Marsais, A. Godard, G. Quéguiner, *J. Chem. Soc., Perkin Trans. 1* **1995**, 2503-2508.

[10] V. Diemer, H. Chaumeil, A. Defoin, A. Fort, A. Boeglin, C. Carré, *Eur. J. Org. Chem.* **2008**, 1767-1776.

[11] a) T. Steiner, *Angew. Chem. Int. Ed.* **2002**, *41*, 48-76; b) X. M. Xiao, M.-A. Haga, T. Matsumurainoue, Y. Ru, A. W. Addison, K. Kano, *J. Chem. Soc., Dalton Trans.* **1993**, 2477-2484; c) G. R. Desiraju, T. Steiner, *The weak hydrogen bond*, Oxford University Press, Oxford, **1999**.

[12] R. M. Silverstein, C. Bassler, T. C. Morrill, *Spectrometric Identification of Organic Compounds, Vol. 5th edition*, Wiley, New York, **1991**.

[13] F. G. Bordwell, J. P. Cheng, *J. Am. Chem. Soc.* **1991**, *113*, 1736-1743.

[14] T. F. Markle, A. L. Tenderholt, J. M. Mayer, *J. Phys. Chem. B* **2012**, *116*, 571-584.

[15] M. Yamaji, J. Oshima, M. Hidaka, *Chem. Phys. Lett.* **2009**, *475*, 235-239.

[16] V. V. Pavlishchuk, A. W. Addison, *Inorg. Chim. Acta* **2000**, *298*, 97-102.

[17] I. Vedernikova, J. P. Tollenaere, A. Haemers, *J. Phys. Org. Chem.* **1999**, *12*, 144-150.

[18] V. W. Manner, T. F. Markle, J. H. Freudenthal, J. P. Roth, J. M. Mayer, *Chem. Commun.* **2008**, 256-258.

[19] a) L. Sacksteder, A. P. Zipp, E. A. Brown, J. Streich, J. N. Demas, B. A. DeGraff, *Inorg. Chem.* **1990**, *29*, 4335-4340; b) L. Wallace, D. P. Rillema, *Inorg. Chem.* **1993**, *32*, 3836-3843; c) K. S. Schanze, D. B. MacQueen, T. A. Perkins, L. A. Cabana, *Coord. Chem. Rev.* **1993**, *122*, 63-89.

[20] J. A. Joule, K. Mills, *Heterocyclic Chemistry, Vol. 3rd edition*, Blackwell Science, Oxford, **2004**.

[21] P. K. Das, M. V. Encinas, J. C. Scaiano, *J. Am. Chem. Soc.* **1981**, *103*, 4154-4162.

[22] M. E. Walther, O. S. Wenger, *Dalton Trans.* **2008**, 6311-6318.

[23] D. M. Roundhill, *Photochemistry and Photophysics of Metal Complexes*, Plenum Press, New York, **1994**.

[24] R. Lomoth, T. Haupl, O. Johansson, L. Hammarström, *Chem.-Eur. J.* **2002**, *8*, 102-110.

[25] T. A. Gadosy, D. Shukla, L. J. Johnston, *J. Phys. Chem. A* **1999**, *103*, 8834-8839.

[26] P. K. Das, M. V. Encinas, S. Steenken, J. C. Scaiano, *J. Am. Chem. Soc.* **1981**, *103*, 4162-4166.

[27] J. T. Kendall, *J. Label. Compd. Radiopharm.* **2000**, *43*, 917-924.

[28] T. Schulz, K. Meindl, D. Leusser, D. Stern, J. Graf, C. Michaelsen, M. Ruf, G. M. Sheldrick, D. Stalke, *J. Appl. Crystallogr.* **2009**, *42*, 885-891.

[29] SAINT v7.68A; Bruker; WI, USA: Madison, 2009.
[30] Sheldrick, G. M. SADABS 2008/2; Göttingen, 2008.
[31] A. Vlcek, F. Bolletta, *Inorg. Chim. Acta* **1983**, *76*, L227-L229.
[32] G. E. Adams, B. D. Michael, *Trans. Faraday Soc.* **1971**, *67*, 1171-1180.

Received: ((will be filled in by the editorial staff))
Published online: ((will be filled in by the editorial staff))

Entry for the Table of Contents

Layout 1:

ARTICLES

Two pyridylphenols with intramolecular hydrogen bonds react with a metal complex via concerted proton-electron transfer: Upon photoexcitation of the complex, there is electron transfer from the phenol to the metal, and the phenolic proton is transferred to the pyridine moiety.

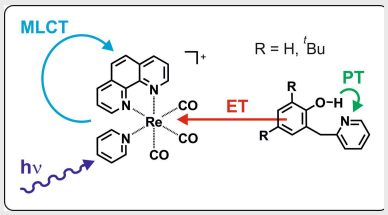

*William Herzog, Catherine Bronner, Susanne Löffler, Bice He, Daniel Kratzert, Dietmar Stalke, Andreas Hauser, Oliver S. Wenger**

Page No. – Page No.

Electron Transfer between Hydrogen-Bonded Pyridylphenols and a Photoexcited Rhenium(I) Complex